


## RESEARCH ARTICLE

# Investigation of Diagnostic Biomarkers for Osteoporosis Based on Differentially Expressed Gene Profile with QCT and mDixon-Quant Techniques

Shan Zhu, MS<sup>1</sup> , Aixian Tian, MS<sup>1</sup>, Lin Guo, MD<sup>1</sup>, Hua Xu, MS<sup>1</sup>, Xiaofeng Li, BS<sup>1</sup>, Zhi Wang, MD<sup>1</sup>, Feng He, PhD<sup>2</sup>

<sup>1</sup>Tianjin Hospital of Tianjin University and <sup>2</sup>Department of Biomedical Engineering, School of Precision Instrument and Optoelectronic Engineering, Tianjin University, Tianjin, China

**Objective:** To develop a comprehensive differential expression profile for osteoporosis based on two independent data sources.

**Methods:** Using a hindlimb unloading (HLU) rat model to mimic osteoporosis syndrome in humans (animal experiments), the significant differentially expressed mRNAs in osteoporosis were analyzed using RNA-seq. The enriched GO terms as well as KEGG signaling pathways were also deeply investigated. Using clinical specimens to verify the functions of potential hub genes (biomarkers) for osteoporosis (clinical experiments), 128 suspected cases for osteoporosis from January 2019 to December 2020 were randomly selected and analyzed by quantitative computed tomography (QCT) as well as modified Dixon quantification (mDixon-Quant) techniques in the Tianjin hospital. Among these, 80 patients out of 128 suspected cases were finally diagnosed as the osteoporosis group. Meanwhile, 48 patients were selected for osteopenia group. There was no significant age and gender difference across participant subgroups. The protein levels of potential hub genes (*FST*, *CCL3*, and *RAPGEF4*) were determined by ELISA double antibody sandwich method for osteopenia and osteoporosis groups from peripheral blood.

**Result:** In the RNA-seq analysis, compared with control group, a total of 803 differentially expressed mRNAs were identified, including 288 up-regulated and 515 down-regulated mRNAs. Of these, *FST*, *CCL3*, *CPE*, *RAPGEF4*, *IL6*, *MDFI*, *PDZD2*, and *GATM* were primary hub genes (biomarkers) for osteoporosis. These differentially expressed genes were significantly enriched in GO terms related to extracellular matrix process and KEGG signaling pathways including osteoclast differentiation. In the functional experiments, the protein expression level of *FST*, *CCL3*, and *RAPGEF4* displayed a specific expression pattern between osteoporosis patients and control group. The protein concentration of *FST* was  $23.63 \pm 6.39$  ng/mL in osteoporosis patients compared as  $48.36 \pm 9.12$  ng/mL in osteopenia group ( $P < 0.01$ ). Meanwhile, *CCL3* was  $1.03 \pm 0.64$  ng/mL in osteoporosis patients vs  $0.56 \pm 0.24$  in osteopenia group ( $P < 0.01$ ) and *RAPGEF4* was  $53.58 \pm 11.42$  ng/mL in osteoporosis patients vs  $66.47 \pm 13.28$  ng/mL in osteopenia group ( $P < 0.05$ ), respectively.

**Conclusion:** This study has identified potential gene biomarkers (the genes with most significantly differential expression and useful for distinguishing osteoporosis from other bone disorders) and established a differential expression profile for osteoporosis, which is a valuable reference for future clinical research.

**Key words:** Differentially expressed gene; HLU rat; mDixon-Quant techniques; Osteoporosis; QCT

**Address for correspondence** Feng He PhD, Department of Biomedical Engineering, School of Precision Instrument and Optoelectronic Engineering, Tianjin University, 92 Wejin road, Nankai district, Tianjin, China 300072; Tel: 18522722391; Email: pufan\_831112@163.com; Zhi Wang MD, Department of Radiology, Tianjin Hospital, No. 406, Jiefangnan road, Hexi district, Tianjin, China 300211; Tel: 13820256789; Email: wz13820256789@163.com

**Grant Sources:** Tianjin Health Science and Technology Project (No. KJ20091, RC20204). Tianjin Science and Technology Project in the Key Field of Traditional Chinese Medicine (No. 2017008).

**Disclosure:** The authors declare no conflict of interest.

Received 25 March 2021; accepted 11 May 2021

## Introduction

Osteoporosis is a systemic bone disease, which is characterized by compromised bone strength that can lead to an increased risk of fracture caused by loss of bone density, bone quality, the destruction of bone microstructure, as well as the increase in bone brittleness<sup>1</sup>. Currently, osteoporosis is one of the major public health problems throughout the world<sup>2</sup>. The social as well as economic burden initiated by osteoporosis has grown rapidly due to the steady increase of the aging population, which comprises the majority of osteoporosis patients. By 2020, it is estimated that approximately 14 mn adults over the age of 50 are affected by osteoporosis worldwide<sup>3</sup>. To date, various factors have been demonstrated as closely associated with the risk of osteoporotic fracture, which include genetical, behavioral, medical as well clinical variables<sup>4</sup>. For instance, it is suggested that low peak bone mass is connected to an increased risk of osteoporotic fracture<sup>5</sup>. Meanwhile, numbers of medical disorders, such as female sex (especially postmenopausal women), BMI < 23 kg/m<sup>2</sup>, diabetes mellitus, malnutrition, a sedentary lifestyle, smoking, excessive alcohol, vitamin D deficiency, lack of sun exposure, hypogonadism with low estrogen and progesterone levels, number of falls, end-organ failure (including cardiac, liver, and renal abnormalities), and preexisting bone mineral abnormalities as well as hypo gonadal states contribute to a considerable amount of osteoporosis cases<sup>6</sup>. At the same time, the long-term use of chemotherapy such as unfractionated heparin (by inhibiting osteoprotegerin and enhancing osteoclastic bone resorption) and coumadin (by inhibiting gamma-carboxylation of osteocalcin) could also depress the bone density of an individual, which is also considered as a potential risk factor.

Osteoporosis is considered as an inevitable symptom of aging. At this moment, a specific chemotherapy for this condition is still lacking, and only basic treatments are available, such as aerobic and resistance exercise associated with a high protein (leucine and creatine) supplement between meals<sup>7</sup>. Clinically, taking Calcium 1000 mg/day and Vitamin D 800 IU/day supplementation, regular weight-bearing exercises for 30 min three times a week, and smoking cessation are recommended for bone loss prevention<sup>8</sup>.

Importantly, osteoporosis is a time-critical emergency, as the disease might progress rapidly, requiring an effective early diagnosis method. The WHO has established a diagnostic criterion for osteoporosis on the basis of bone mass density (BMD) T-scores<sup>9</sup>. Due to the complexity of BMD T-scores, other imaging methods have been generated for osteoporosis. DXA and quantitative computed tomography (QCT) are the primary administrations popularly utilized in clinic<sup>10</sup>. Additionally, some potential biomarkers have been initiated in clinical research gradually, which are generally released from osteoblasts and typically are measured in serum<sup>11</sup>. For instance, the bone-specific alkaline phosphatase (BSAP) as well as osteocalcin have been testified for osteoporosis diagnosis<sup>12</sup>. At the same time, the bone turnover markers have been initiated recently for postmenopausal

osteoporosis<sup>13</sup>. This is based on the fact that the process of bone turnover includes two independent processes: the removal of old bone (resorption) as well as the laying down of new bone (formation). The N-terminal propeptides of type I procollagen (PINP) and C-telopeptide of type I collagen (CTX-I) have been suggested as the markers of bone formation and resorption, which have been recommended for clinical use already. However, the application of these markers is still controversial. First of all, these markers seem to be solely for postmenopausal women, not for all the individuals. Moreover, these markers are subject to several sources of variability, such as feeding conditions (resorption decreases) and recent fracture (all markers increase for several months). At the same time, these markers are not useful for diagnosis of osteoporosis and do not improve prediction of bone loss or fracture within an individual. To this end, more studies are necessary to explore the use of bone turnover markers for assessment of the bone safety of new medications. In summary, due to missing tissue specificity, the sensitivity of these biomarkers are still inferior and they provide limited applications in the diagnosis of osteoporosis as well as the prediction of bone mass. Overall, the diagnosis, which depends on biomarkers, is emerging as the major obstacle for osteoporosis study.

Based on inflated misdiagnosis rates and poor accuracy of diagnosis, osteoporosis has been difficulty to treat clinically. In addition, the efficiency of biomarkers used in clinic is far from satisfactory. Therefore, it is urgent to establish a differentially expressed profile of potential biomarkers (the genes with most significantly differential expression and useful for distinguishing osteoporosis from other bone disorders) for osteoporosis. At this moment, there is a lack of public resources for human osteoporosis, such as the GEO or TCGA database. To this end, we established an osteoporosis rat model and the differentially expressed genes were explored by RNA-seq and bioinformatics methods. Of the potential biomarkers, the most significant were further investigated and confirmed in clinic using human osteoporosis patient serums. All of these promising outcomes enriched the early diagnosis of the disease, which provided great help for osteoporosis study.

## Material and Methods

### Animal Experiments

#### Animal Handling

All the animal procedures were conducted according to the National Institutes of Health guide for the administration and utilization of laboratory animals. The protocol developed in the study was initially approved by the Animal Care and Use Committee of Tianjin Hospital (2019012). The male 12-week-old Sprague Dawley (SD) rats were housed individually in a standard temperature-controlled, specially designed animal facility using a procedure of 12:12 h light:dark cycle and free access to chow diet and water.

### Hindlimb Suspension Procedure

The osteoporosis in rats was successfully generated by hindlimb unloading (HLU) model procedure, where the immobilization symptoms were achieved by tail suspension, as previously established<sup>14,15</sup>. In the process, the tail of HLU rat was washed completely using 70% isopropanol and subsequently coated using benzoin solution. After that, a strip of adhesive tape was applied to the tail, which was suspended by passing the tape through a fish-line swivel. The swivel was normally connected with a metal bar on the top of the cage. The forelimbs of the rat were allowed to touch the grid floor so that it could move around as well as freely access to food and water. The suspension height was adjusted every day accordingly, which was mainly to prevent the hindlimbs from touching the supporting surface to maintain a suspension angle of approximately 30°<sup>16</sup>. The rats used for the HLU groups and the normal control groups were sacrificed at day 28 (10 rats each), respectively. Bones of the lower extremities were collected for subsequent experiments.

### Micro-Computed Tomography ( $\mu$ CT) Scan

The left femurs of both groups of rats were scanned using  $\mu$ CT (Skyscan 1276, Bruker microCT, Kontich, Belgium) for the high-quality images of the trabecular and cortical bone. The scanning parameters were finally set as follows: 17.5  $\mu$ m spatial resolution, 70 kV, 200  $\mu$ A, and 498 ms of integration time. The length of region of interest (ROI) was 1977  $\mu$ m, starting from 262  $\mu$ m proximal to the distal epiphyseal plate of the femur. The trabecular microarchitecture of the two groups were compared with the following values: bone volume fraction (bone volume/total volume, BV/TV), trabecular thickness (Tb.Th), trabecular number (Tb.N), as well as trabecular separation (Tb.Sp).

### RNA-seq

High-throughput sequencing service was provided by Cloudseq Biotech (Shanghai, China). High-throughput sequencing and subsequent bioinformatics analysis of the transcriptome were performed by Cloud Seq Biotech (Shanghai, China). To put it simply, the Ribo Zero rRNA elimination Kit (Illumina, US) was developed to remove total RNA, according to the manufacturer's instructions. The RNA library was constructed by means of rRNA-depleted RNA samples with the TruSeq Stranded Total RNA Library Prep Kit (Illumina, USA). The quality analysis and quantification of the library were developed on the bioanalyzer 2100 system (Agilent Technologies, USA). The 10 pM libraries were denatured into single-stranded DNA molecules, captured on Illumina flow cells, amplified *in situ* in the form of clusters, and 150 cycles of sequencing were performed on the Illumina Hiseq sequencer according to the manufacturer's instructions.

### Differential Gene Analysis

The limma package in R language was developed to analyze the differentially expressed mRNAs between different groups, taking the absolute value of the log-transformed differential

expression multiple (Log2FC) > 1 and *P*-value < 0.05 as standards for analysis.

### Functional Enrichment Analysis

For the obtained differentially expressed genes, we used the "clusterProfiler" function package in R language for enrichment analysis of GO (including Biological Process, Molecular Function, and Cellular Component) and KEGG Pathway. When *P*-value < 0.05, we considered the corresponding entries to be significantly enriched.

### Protein-Protein Interaction (PPI) Networks

The STRING database is a database for the functional protein-protein interaction analysis and prediction<sup>17</sup>, of which the interaction pairs with a combined score greater than or equal to 0.4 (confidence score  $\geq$  0.4) were retained. At the same time, the Cytoscape (<https://cytoscape.org/>, version 3.7.2) was developed to visualize the PPI network<sup>18</sup>. The molecular complex detection method (MCODE) was plugged in Cytoscape software to identify the significantly functional clustering modules, with the MCODE score > 2 as a threshold.

### Clinical Experiments

#### Imaging Analysis

A total of 128 suspected cases for osteoporosis from January 2019 to December 2020 were randomly selected and analyzed by quantitative computed tomography (QCT) as well as modified Dixon quantification (mDixon-Quant) techniques in the Tianjin hospital.

The inclusion criteria were as following: (i) age: 40–70 years; (ii) suspected case for osteoporosis.

The exclusion criteria were as following: (i) other existing orthopaedic disease; (ii) existing blood diseases and tumors; (iii) refusal to sign the informed consent.

This study was in line with the medical ethics standards and approved by the hospital ethics committee. All treatment and testing were performed only when informed consent of patients or their families were received. Using these criteria, 80 patients out of 128 suspected cases were finally diagnosed as osteoporosis group. At the same time, 48 patients were selected for osteopenia group. There was no significant age and gender difference across participant subgroups. The characteristics of participants recruited for the study is shown in Table 1.

**TABLE 1** Characteristics of participants recruited for the study

Group	Case	Age (year)	Gender	
			Male	Female
Osteopenia	48	53.16 $\pm$ 4.48	26	22
Osteoporosis	80	56.38 $\pm$ 5.02	45	35
<i>t</i> or $\chi^2$		0.16		2.58
<i>P</i>		0.19		0.11

### Lumbar Vertebral Bone Marrow Fat Content Measurement

The fat content was measured with Ingenia 3.0 TMR scanner (Philips Healthcare), with a 32-channel body coil, 6-echo mDixon-Quant gradient echo sequence, sagittal scan. The parameters were set up as follows: TR, 5.6 ms; TE, 0.98 ms;  $\Delta$ TE, 0.7 ms; flip angle, 3°; voxel, 2.5 mm  $\times$  2.5 mm  $\times$  3 mm; matrix, 160  $\times$  140; excitation frequency, one time; layer thickness, 3 mm; FOV, 400 mm  $\times$  350 mm  $\times$  231 mm; scanning time, 15 s. All data was transferred to the post-processing workstation using ISP software (version 7, Philips Healthcare), automatically generating fat score images for measurement. The most central image of the lumbar spine in the sagittal position was selected for the region of interest (ROI) on the L1-L3 vertebral body. The ROI required the largest range to be included in the entire vertebral body as well as avoid the cortical bone, endplate and intervertebral disc. All measurements were performed independently by two residents, and the average value of the measurements was taken.

### Quantitative CT (QCT) Diagnostic Criteria for Osteoporosis

The criteria was based on the diagnostic standard of the International Society for Clinical Bone Density: QCT average BMD  $> 120 \text{ mg/cm}^3$  as normal;  $80\sim 120 \text{ mg/cm}^3$  as bone loss while  $< 80 \text{ mg/cm}^3$  as diagnose osteoporosis.

### QCT Bone Mineral Density (BMD) Measurement

The low-dose thoracic CT and QCT BMD measurements were performed by GE 16-row CT on the upper edge of the first lumbar spine (L1) to the lower edge of the third lumbar spine (L3). The CT scanning images were transmitted to the QCT-BMD measuring station (mindways), and the ROI was marked in the cancellous bone regions of L1, L2, and L3 vertebral bodies respectively.

### ELISA Investigation for Biomarkers

The patients were divided into two groups based on previous standard: osteoporosis group (80 patients) and osteopenia group (48 patients).

The concentrations of potential biomarkers (*FST*, the antibody purchased from Abcam 232761; and *CCL3*, the antibody purchased from Abcam 1796381 as well as *RAPGEF4*, the antibody purchased from Abnova H00011069-M01) were determined by the ELISA double antibody sandwich method, and the specific operation was carried out in strict accordance with the kit instructions (purchased from Abcam). The samples were freshly prepared and extracted from the peripheral blood of patients in different groups. Dilution process was followed with standard protocol: the standard wells were set up on the enzyme-labeled coating plate; 100  $\mu\text{L}$  of standard products was added to the first and second wells, following 50  $\mu\text{L}$  of standard diluent (PBS); the volume of each well was maintained at 50  $\mu\text{L}$ ,

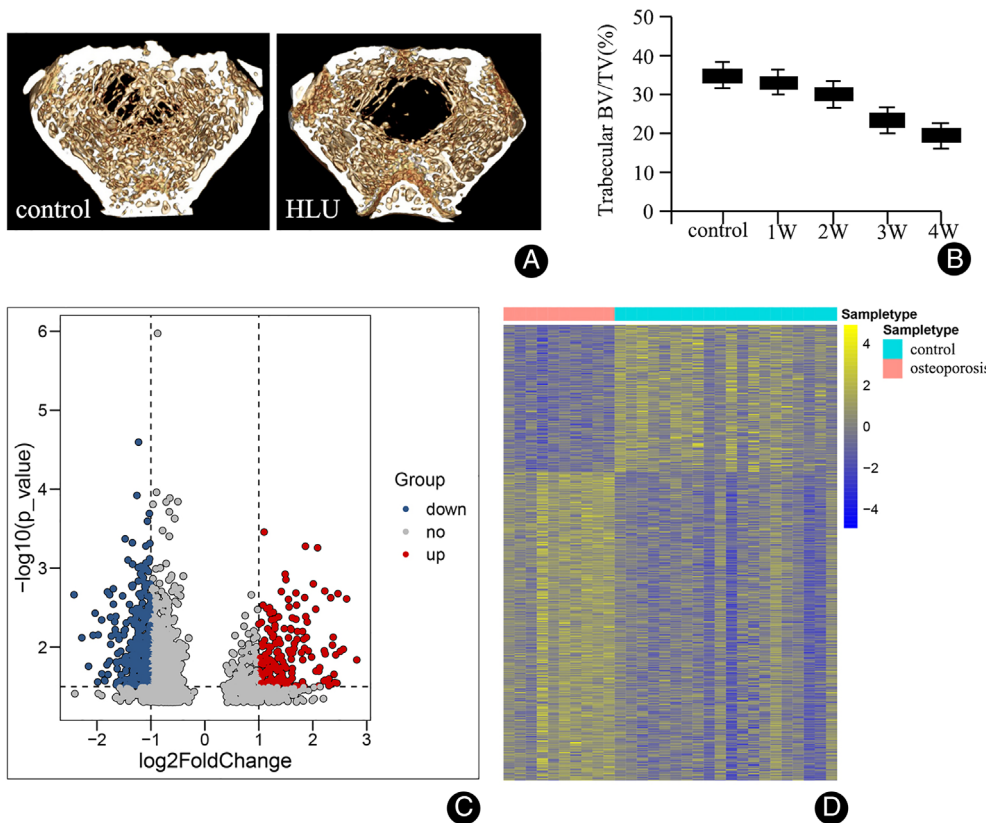


**Fig 1** Analysis of differentially expressed genes for osteoporosis using HLU rat. (A) Representative  $\mu\text{CT}$  images in cross-sectional plane in rat distal femur after 4 weeks of HLU ( $n = 6$ ). (B) Trabecular BV/TV analysis of distal femur ( $n = 6$ ). (C) The volcano map of differentially expressed mRNAs between two groups. The horizontal axis represents the multiple of differential expression ( $\text{Log}_2\text{FC}$ ), the vertical axis represents  $-\log_{10}(\text{FDR})$ . The red dots indicate up-regulated genes, and the blue dots indicate down-regulated genes. (D) The heat map of differentially expressed mRNAs. The horizontal axis represents sample, vertical axis represents different gene.



which generated series concentration as 24, 16, 8, 4, and 2  $\mu\text{g/L}$ ; the blank control wells were performed without samples and enzyme-labeled reagents. The 10  $\mu\text{L}$  of the sample was gently mixed with 40  $\mu\text{L}$  of dilutant from each standard well, which was subsequently evaluated on the enzyme-labeled coated plate. The mixture was sealed and incubated at 37°C for 30 min. Afterward, the liquid was discarded, and the wells were spun dry following five thorough washes with washing solution. The 50  $\mu\text{L}$  of enzyme-labeled reagent was added to each well, except for blank control, with another incubation and wash. For the development of color, a combination of 50  $\mu\text{L}$  of color developer A and B was added to each well. The mixture was shaken gently and mixed well following a color development at 37°C for 30 min. A total of 50  $\mu\text{L}$  of stop solution was applied to terminate the reaction. The final concentration of each biomarker was measured by the absorbance (OD value).

### Statistical Analysis

The data was established using Excel 2013 software database, following processing with SAS 9.4 and SPSS 19.0 statistical software data analysis. The continuous variables were tested by normal distribution, which were expressed as Mean  $\pm$  SD. The student *t*-test in SAS 9.4 was used for data comparison as the  $P < 0.05$  indicated the significant difference.

### Results

#### Characterization of Osteoporosis in HLU Rat Model and Differentially Expressed Gene Analysis

In this study, the HLU rat model was generated to mimic osteoporosis syndrome. The trabecular bone in the distal femur declined gradually at time of HLU, shown as the  $\mu\text{CT}$  images as well as trabecular BV/TV ratio of distal femur (Fig. 1A,B). The rats from control and HLU groups at week

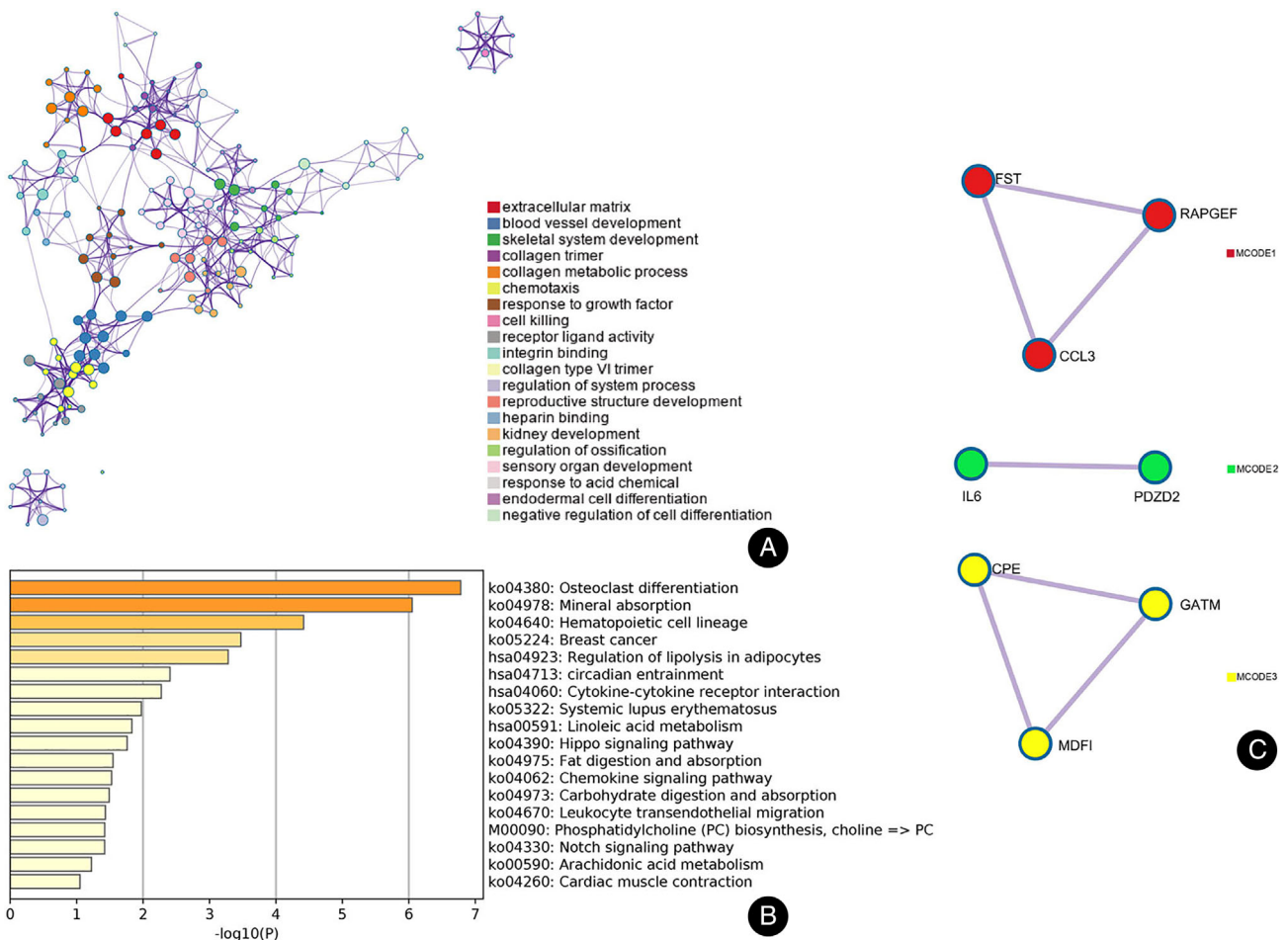


**Figure 2** GC and KEGG enrichment results for osteoporosis. (A) The top GO term enrichment results with the largest number of genes. The horizontal axis represents the number of enriched genes and the vertical axis represents the name of each GO term. (B) The enrichment results of the KEGG pathways with the largest number of genes. The horizontal axis in the figure indicates the number of genes enriched, and the vertical axis indicates the name of each KEGG pathway. (C) The PPI network for the potential target genes for osteoporosis.

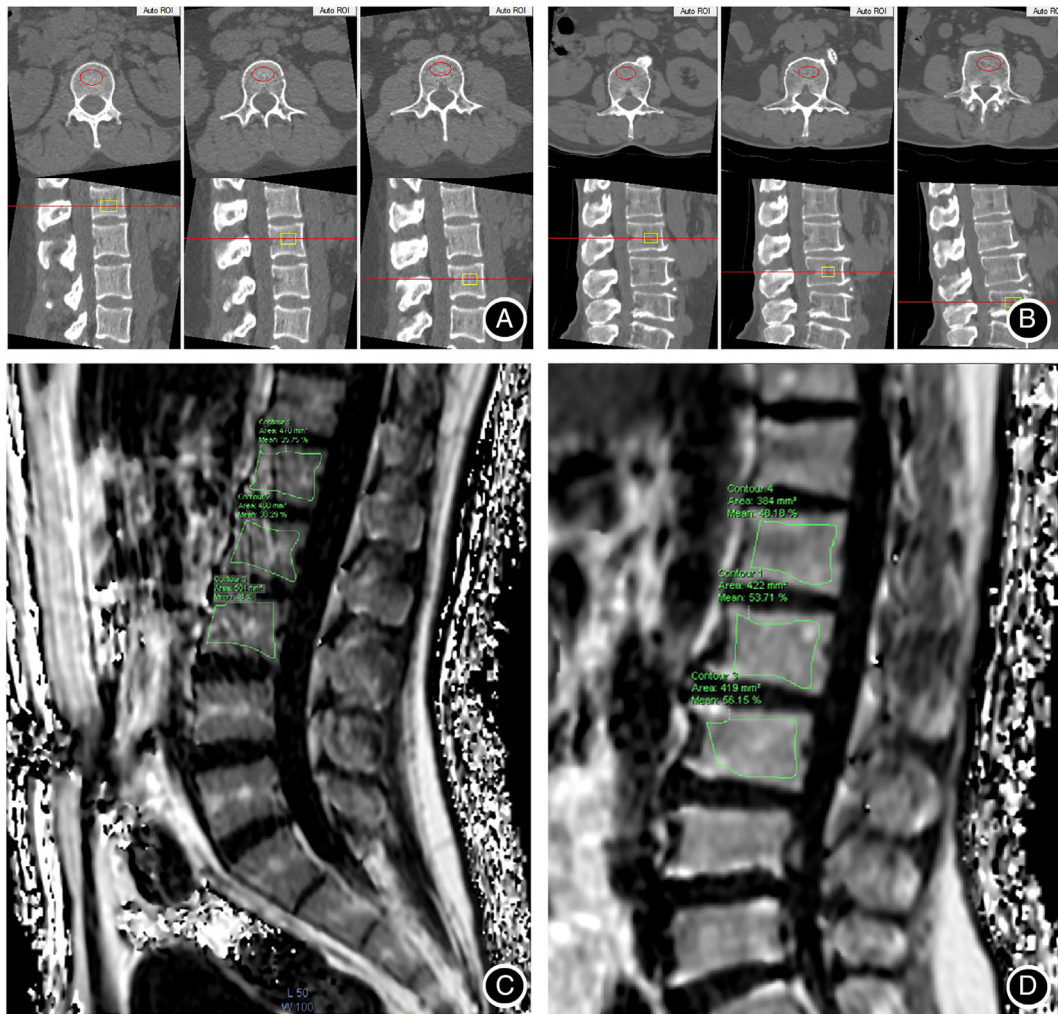


**Fig 3** Clinical diagnosis of osteoporosis patients using imaging methods. (A, B) The QCT imaging for control and osteoporosis patients respectively. (C, D) The comparison between control and osteoporosis patients using mDixon-Quant techniques.

4 were selected for the RNA library establishment. Based on the differential analysis, osteoporosis group (HLU rat) demonstrated 803 differentially expressed mRNAs, with 288 up-regulated ones and 515 down-regulated ones (Fig. 1C,D) compared with control group. Of these, *FST*, *CCL3*, *CPE*, *RAPGEF4*, *IL6*, *MDFI*, *PDZD2*, and *GATM* were primary hub genes (biomarkers) for osteoporosis (with most significant difference between two groups).

#### Enrichment Analysis Results and Protein–Protein Interaction (PPI) Analysis

By performing GO and KEGG enrichment analysis on these 803 differentially expressed mRNAs, it could be suggested that these differentially expressed genes were significantly enriched in GO terms related to extracellular matrix process (Fig. 2A) and the KEGG signaling pathways including osteoclast differentiation, mineral absorption, and so on (Fig. 2B).

**TABLE 2** Selected gene concentrations were compared between osteopenia and osteoporosis groups

	FST (ng/mL, x ± s)	CCL3 (ng/mL, x ± s)	RAPGEF4 (ng/mL, x ± s)
Osteopenia group	48.36 ± 9.12	0.56 ± 0.24	66.47 ± 13.28
Osteoporosis group	23.63 ± 6.39	1.03 ± 0.64	53.58 ± 11.42
t	7.06	6.86	1.37
P	<0.01	<0.01	<0.05

The STRING database was processed to construct a PPI network for potential hub genes. The MCODE plug-ins here indicated three significant clustering modules (Fig. 2C). The cluster 1 included *FST*, *CCL3*, and *RAPGEF4* genes. *IL6* and *PDZD2* contributed to cluster 2, while *CPE*, *MDFI*, and *GATM* composed cluster 3, respectively. These eight genes were shown to be the key target genes for osteoporosis formation.

### **Clinical Diagnosis of Osteoporosis Using Imaging Techniques**

A total of 128 suspected cases for osteoporosis were further investigated using QCT and mDixon-Quant techniques. These methods could efficiently distinguish between osteoporosis and osteopenia patients (Fig. 3). With the double insurance plan, 80 patients were finally diagnosed as osteoporosis group for the subsequent analysis.

### **External Verification of Hub Gene Functions for Osteoporosis**

Next, we sought to verify the functions of hub genes as biomarkers for osteoporosis diagnosis. Since genes in cluster 1 showed a promising difference between two groups by the RNA-seq, we studied the protein expression level of *FST*, *CCL3*, and *RAPGEF4* using ELISA method. As indicated in Table 2, the protein concentration of *FST* was  $23.63 \pm 6.39$  ng/mL in osteoporosis patients compared as  $48.36 \pm 9.12$  ng/mL in osteopenia group ( $t = 7.06$ ,  $P < 0.01$ ). Meanwhile, *CCL3* was  $1.03 \pm 0.64$  ng/mL in osteoporosis patients vs  $0.56 \pm 0.24$  in osteopenia group ( $t = 6.86$ ,  $P < 0.01$ ) and *RAPGEF4* was  $53.58 \pm 11.42$  ng/mL in osteoporosis patients versus  $66.47 \pm 13.28$  ng/mL in osteopenia group ( $t = 1.37$ ,  $P < 0.05$ ), respectively. These outcomes suggested that these three genes could be latent biomarkers for osteoporosis patients in clinic.

## **Discussion**

### **Effective Biomarkers are Required for Osteoporosis**

Osteoporosis has been currently acknowledged as the most prevalent bone disorder in the world, especially for elder people. In the normal situation, the amount of bone lost should be equal to the amount of new bone formed. However, when this balance becomes “uncoupled”—as the consequence of aging, unbalance of hormones, changes in serum calcium levels—there is a net loss of bone, which is the initiation of osteoporosis. To date, osteoporosis is recommended by the world health organization (WHO) as a T-score of  $-2.5$  standard deviations (SD) below the BMD of a healthy younger person of the same sex<sup>19</sup>. The calculation of BMD as well as diagnosis of osteoporosis mainly depend on the techniques of dual energy X-ray absorptiometry (DXA)<sup>20</sup>. Nowadays, researchers have been trying to find breakthroughs in the early screening and diagnosis of osteoporosis and have made considerable progress in these areas, but the effect is far from satisfactory<sup>21</sup>. On one hand, the current imaging detection technology inevitably has human errors, which has contributed to a high misdiagnosis rate. On other hand, due to incidence of osteoporotic fracture increases with advancing age, the prevention of osteoporosis is a primary public health concern worldwide. Unfortunately, only a small proportion of the elderly population pay attention to the imaging analysis for osteoporosis during a routine physical examination. For this purpose, an effective biomarker

based on the differentially expressed gene profile is a top priority.

### **Investigation of Differentially Expressed Genes for Osteoporosis**

At this moment, a public open resource for human osteoporosis is still missing, like GEO or TCGA database. Therefore, we established an osteoporosis animal model using HLU rat. HLU rat had been previously established in our laboratory, which is a well-accepted animal model for dysmotility syndrome including osteoporosis<sup>17,22</sup>. Using this innovative model, it could be demonstrated that 803 genes displayed a specific expression pattern between control and osteoporosis groups (Fig. 1). Under the normal circumstance, adult bone mass results from peak during adolescence and is subsequently maintained until perturbations in the bone process of remodeling cycle. This well-regulated procedure is balanced between bone-forming osteoblasts and bone-resorbing osteoclasts<sup>23</sup>. Therefore, it was reasonable to speculate these differentially expressed genes were enriched in GO terms related to extracellular matrix process and the KEGG signaling pathways including osteoclast differentiation (Fig. 2). Among these candidates, eight primary hub genes including *FST*, *CCL3*, *CPE*, *RAPGEF4*, *IL6*, *MDFI*, *PDZD2*, and *GATM* were subdivided into three clusters by PPI investigation. *FST* stands for TGF- $\beta$  superfamily antagonist follistatin, therapy dose-dependently of which increased cancellous bone mass up to 42% and improved bone microstructural indices in mice<sup>24</sup>. Actually, various inhibitors of the activin receptor signaling pathway (IASPs), like *FST*, have become the latent therapeutics for some bone remodeling disorders based on their ability to increase muscle and bone mass.

### **Potential Hub Genes were Confirmed by External Clinical Experiments**

Since the differentially expressed genes were hypothesized from rat tissue, whether they presented the same results in human being was an important concern for us. To this end, we performed an ELISA assay using osteoporosis patients (shown in Table 1). In a study by Farangis *et al.*, the circulating chemokines were detected by ELISA immediately after blood collection according to the manufacturer's guidelines for control and osteoporosis patients. Similar to the results here, three members of *CCL* including *CCL2*, *CCL3*, as well as *CCL5* were elevated in osteoporosis patients<sup>25</sup>, whereas the mean contents of *CCL3* were  $(936.39 \pm 204)$  pg/mL and  $(134.5 \pm 4.58)$  pg/mL in osteoporosis patients and controls, respectively. They claimed that *CCL3*, through binding to *CCR1* and *CCR5*, could stimulate *CCL5* secretion from osteoblasts. Since *CCL5* manipulates several important osteoclast functions and *CCL3* is secreted predominantly by osteoclasts, it is meaningful to hypothesize that communication between osteoclasts and osteoblasts could be regulated by these two chemokines.

### Limitations of the Study

Certain limitations should be acknowledged in this study. For instance, one significant aspect was that the differentially expressed gene profile was generated from rat model, which clear initiated a concern about extra-species differences. Second, even though we performed a PPI analysis for the hub gene interactions, the internal connections between these genes and osteoporosis have not been fully explored yet, which required *in vivo* study for further verification Third, external verification of hub gene functions for osteoporosis was collected from only one hospital. The sample size was limited. To further develop the clinical application, more participants including different gender and personality traits should be recruited in the study. To address these issues, we would take further steps and more efforts to consider the aspects mentioned above.

### Conclusion

In conclusion, in the light of the fact that there remains no gold standard clinical diagnostic biomarkers for osteoporosis patients, we established a comprehensive expression profile for osteoporosis using HLU rat model. Several potential biomarkers were initiated and verified by clinical osteoporosis specimen. Overall, we shed light on questions and challenges posed by osteoporosis, and provide tremendous help for future understanding of the disease.

### Authorship Declaration

All authors listed meet the authorship criteria according to the latest guidelines of the International Committee of Medical Journal Editors, and all authors are in agreement with the manuscript.

### Reference

1. Brown C. Osteoporosis: staying strong. *Nature*, 2017, 550: S15–S17.
2. Ensrud KE, Crandall CJ. Osteoporosis. *Ann Intern Med*, 2017, 167: ITC17–ITC32.
3. Srivastava M, Deal C. Osteoporosis in elderly: prevention and treatment. *Clin Geriatr Med*, 2002, 18: 529–555.
4. Lane NE. Epidemiology, etiology, and diagnosis of osteoporosis. *Am J Obstet Gynecol*, 2006, 194: S3–S11.
5. Mora S, Gilsanz V. Establishment of peak bone mass. *Endocrinol Metab Clin North Am*, 2003, 32: 39–63.
6. Aspray TJ, Hill TR. Osteoporosis and the ageing skeleton. *Subcell Biochem*, 2019, 91: 453–476.
7. Bandeira L, Bilezikian JP. Novel therapies for postmenopausal osteoporosis. *Endocrinol Metab Clin North Am*, 2017, 46: 207–219.
8. Cotts KG, Cifu AS. Treatment of osteoporosis. *JAMA*, 2018, 319: 1040–1041.
9. WHO Study Group. Assessment of fracture risk and its application to screening for postmenopausal osteoporosis. *World Health Organ Tech Rep Ser*, 1994, 843: 1–129.
10. Miller PD. Management of severe osteoporosis. *Expert Opin Pharmacother*, 2016, 17: 473–488.
11. Eastell R, Szulc P. Use of bone turnover markers in postmenopausal osteoporosis. *Lancet Diabetes Endocrinol*, 2017, 5: 908–923.
12. Fassbender WJ, Steinhauer B, Stracke H, Schumm-Draeger PM, Usadel KH. Validation of a new automated immunoassay for measurement of intact osteocalcin. *Clin Lab*, 2002, 48: 31–38.
13. Crandall CJ, Ensrud KE. Osteoporosis screening in younger postmenopausal women. *JAMA*, 2020, 323: 367–368.
14. Li B, Liu J, Zhao J, et al. LncRNA-H19 modulates Wnt/beta-catenin signaling by targeting Dkk4 in hindlimb unloaded rat. *Orthop Surg*, 2017, 9: 319–327.
15. Li B, Zhao J, Ma J, et al. Overexpression of DNMT1 leads to hypermethylation of H19 promoter and inhibition of Erk signaling pathway in disuse osteoporosis. *Bone*, 2018, 111: 82–91.
16. Li B, Zhao J, Ma J, et al. Cross-talk between histone and DNA methylation mediates bone loss in hind limb unloading. *J Bone Miner Res*, 2021, 36: 956–967.
17. Szklarczyk D, Gable AL, Lyon D, et al. STRING v11: protein-protein association networks with increased coverage, supporting functional discovery in genome-wide experimental datasets. *Nucleic Acids Res*, 2019, 47: D607–D613.
18. Shannon P, Markiel A, Ozier O, et al. Cytoscape: a software environment for integrated models of biomolecular interaction networks. *Genome Res*, 2003, 13: 2498–2504.
19. Coughlan T, Dockery F. Osteoporosis and fracture risk in older people. *Clin Med (Lond)*, 2014, 14: 187–191.
20. Johnston CB, Dagar M. Osteoporosis in older adults. *Med Clin North Am*, 2020, 104: 873–884.
21. Khosla S. Personalising osteoporosis treatment for patients at high risk of fracture. *Lancet Diabetes Endocrinol*, 2019, 7: 739–741.
22. Zhang ZK, Li J, Guan D, et al. A newly identified lncRNA MAR1 acts as a miR-487b sponge to promote skeletal muscle differentiation and regeneration. *J Cachexia Sarcopenia Muscle*, 2018, 9: 613–626.
23. Reid IR. A broader strategy for osteoporosis interventions. *Nat Rev Endocrinol*, 2020, 16: 333–339.
24. Lodberg A, van der Eerden BCJ, Boers-Sijmons B, et al. A folistatin-based molecule increases muscle and bone mass without affecting the red blood cell count in mice. *FASEB J*, 2019, 33: 6001–6010.
25. Fatehi F, Mollahosseini M, Hassanshahi G, et al. CC chemokines CCL2, CCL3, CCL4 and CCL5 are elevated in osteoporosis patients. *J Biomed Res*, 2017, 31: 468–470.